Advances in Materials Research, *Vol. 13, No. 5 (2024) 355-374*
https://doi.org/10.12989/amr.2024.13.5.355

Analytical model of stress-strain curve for foamed cellular concrete in compression

Facundo A. Retamal* and Viviana C. Rougier[a]

Computational Mechanics and Structures Research Group (GIMCE), Civil Engineering Department, C. del Uruguay Regional Faculty (FRCU), National Technological University (UTN), Argentina

(*Received August 18, 2022, Revised October 13, 2022, Accepted April 18, 2024*)

Abstract. Several mathematical models describe the compressive behaviour of different types of concretes, but no specific one for foamed cellular concrete (FCC) has been developed. In this work, simple compression tests on FCC specimens of different mixes were conducted to study this material's compression behaviour curve until failure. Using continuous load and displacement measurement equipment, it was possible to obtain stress-strain curves up to peak for FCC of different strengths (from 1.20 to 47.34 MPa). Elastic modulus, compressive strength and failure strain values were also determined. Through the analysis of the mentioned curves, a mathematical model of them was obtained, through which it is possible to describe the compression behaviour of FCC up to failure. The comparison between the predicted curve against experimental data shows the effectiveness of the proposed model.

Keywords: experimental campaign; foamed cellular concrete; mathematical model development; porosity; strength prediction model

1. Introduction

Foamed cellular concrete (FCC) is a lightweight concrete (LC) that can reach highly variable densities, normally between 300 and 2100 kg/m^3. It is made up of a cement mixture, which can be a cement paste or mortar, with the incorporation of air bubbles through a pre-formed foam (ACI 2014a). It is also common to incorporate active or inert mineral additions, chemical additives, and fibres, among others, which can accompany or replace all or part of the base materials (Amran *et al.* 2015). Because of these facts, it's a material with particular and highly variable characteristics, depending on the use for which it is designed (Retamal and Rougier 2022).

FCC has interesting characteristics for its application in the construction industry, such as its low weight, high workability, and fluidity, and depending on its design it can be self-compacting. Besides, it has high thermal and water-repellent insulation, and adequate fire resistance, among others (Narayanan and Ramamurthy 2000). Through its mix design, variable characteristics can be achieved. In the mechanical issue, compressive strengths from less than 1 MPa to values greater than 40 MPa have been obtained (Jones and McCarthy 2005, Chica and Alzate 2019); elastic modules between 1 and 12 MPa (Brady *et al.* 2001), and similar occurs with the rest of the material

*Corresponding author, Professor, E-mail: retamalf@frcu.utn.edu.ar
[a]Professor, E-mail: rougierv@frcu.utn.edu.ar

http://www.techno-press.org/?journal=amr&subpage=5 ISSN: 2234-0912 (Print), 2234-179X (Online)

properties. In the last years, the knowledge about FCC and its mechanical characteristics has been notably increasing and, with this, its use in structural elements (Amran *et al.* 2015, Jones and McCarthy 2005, Retamal and Rougier 2024).

This paper presents a contribution to the study of the use of FCC applied to resistant elements, through the development of a stress-strain curve model, which describes its behaviour in simple compression, up to failure, without confinement. It's a continuation and improvement of previously published work of the authors in this topic (Retamal and Rougier 2021).

Different kinds of mathematical models are developed by researchers for optimizing the design of structural elements and improving cost-effectiveness among other important building decision-making (Alshboul *et al.* 2022b, Almasabha *et al.* 2022, Alshboul *et al.* 2022a, Tarawneh *et al.* 2021). A mathematical model of stress-strain curve allows the description of the material mechanical behaviour under a certain effort, by the input of a smaller number of data, and so, they are necessary for their numerical modelling (Sun *et al.* 2018), among other important functions. In the case of concrete, several models have been developed for different types, such as normal concrete (NC), LC, high strength concrete (HSC), fibre reinforced concrete, etc. (Lim and Ozbakkaloglu 2014, Popovics 1973, Sargin *et al.* 1971, Lu and Zhao 2010).

Concrete stress-strain relationship models can be divided into 2 groups, based on their mathematical expression (Lu and Zhao 2010): those based on the Popovics (1973) expression, and those based on Sargin *et al.* (1971) model. Several modifications have been made to these models over the years, to adapt them to other types of concrete. Mainly, work has been done proposing various expressions to obtain the parameters of the curve, such as strain at peak stress, the elastic modulus of the material, etc. (Lim and Ozbakkaloglu 2014).

Published in 1973, Sandor Popovics' model (Popovics 1973), is an appropriate expression to estimate the complete diagram of the stress-strain relationship for NC, when the compressive strength of the concrete and its corresponding specific strain are known, as input data. The expression is presented in Eq. (1), where: f_0 is the maximum compressive stress of the concrete, ε_0 the specific strain corresponding to this stress value, f the compressive stress at a given point on the curve and ε its corresponding value of specific deformation, and β is a factor used to modify the shape of the curve, adapting it to different types of concrete. Popovics proposed expressions for β for concrete, mortar, and cement paste. This model gives a good approximation of the curve also for low-resistance concrete and considers the increase in the value of the specific deformation at the material's stress peak as its resistance increases (Popovics 1973).

$$\frac{f}{f_0} = \left(\frac{\varepsilon}{\varepsilon_0}\right) \frac{\beta}{\beta - 1 + \left(\varepsilon/\varepsilon_0\right)^{\beta}} \tag{1}$$

Tomaszewicz (1984) proposed the incorporation of the coefficient k to Popovics' model, which is a function of the compressive strength of the concrete, to describe the unloading stage of the curve. He also proposed new values for the determination of the elastic modulus of the concrete and for the β factor. The mathematical expression for this model is shown in Eq. (2).

$$\frac{f}{f_0} = \left(\frac{\varepsilon}{\varepsilon_0}\right) \frac{\beta}{\beta - 1 + \left(e/e_0\right)^{k\beta}} \tag{2}$$

Carreira and Chu (1985), proposed new expressions for E, ε_0 and β. Later, Hsu and Hsu (1994), published their stress-strain relationship model, shown in Eq. (3). They modified the Carreira and Chu model by incorporating the coefficient n, which takes on different values depending on the compressive strength of the concrete, and a new expression of β to adapt the curve to the behaviour

of the HSC with and without confinement.

$$\frac{f}{f_0} = \left(\frac{\varepsilon}{\varepsilon_0}\right) \frac{n\beta}{n\beta - 1 + \left(\varepsilon/\varepsilon_0\right)^{n\beta}} \tag{3}$$

Wee *et al.* (1996), modified the model of Hsu and Hsu replacing the factor n by the parameters k_1 and k_2, which are functions of the compressive strength of the concrete introduced. The expression of the curve is shown in Eq. (4).

$$\frac{f}{f_0} = \left(\frac{\varepsilon}{\varepsilon_0}\right) \frac{k_1\beta}{k_1\beta - 1 + \left(\varepsilon/\varepsilon_0\right)^{k_2\beta}} \tag{4}$$

Later, Lim and Ozbakkaloglu (2014), proposed another stress-strain model, in the line of Popovics' one, for NC and LC, through a large literature review and a statistic analysis applied to the data collected. They modified the mathematical expression that defines the β coefficient and adapted the model for confined and unconfined concrete.

In 1971, Sargin *et al.* (1971), published their compression stress-strain curve model for concrete, which is shown in Eq. (5), giving rise to the other group of mentioned mathematical expressions. The A factor was introduced, which is a function of the compressive strength of the material, of the specific deformation corresponding to this stress value, and of the elastic modulus of the material. The D factor depends only on f_0, and he also proposes expressions for the determination of E and ε_0.

$$f = f_0 \left[\frac{A\left(\frac{\varepsilon}{\varepsilon_0}\right) + (D-1)\left(\frac{\varepsilon}{\varepsilon_0}\right)^2}{1 + (A-2)\left(\frac{\varepsilon}{\varepsilon_0}\right) + D\left(\frac{\varepsilon}{\varepsilon_0}\right)^2}\right] \tag{5}$$

Wang *et al.* (1978), proposed their model based on the expression of Sargin *et al.*, but considering a series of 4 factors A, B, C and D, as shown in Eq. (6). There, 2 groups of factors are used, one to describe the ascending portion of the curve and the other for the descending one.

$$f = f_0 \left[\frac{A\left(\frac{\varepsilon}{\varepsilon_0}\right) + B\left(\frac{\varepsilon}{\varepsilon_0}\right)^2}{1 + C\left(\frac{\varepsilon}{\varepsilon_0}\right) + D\left(\frac{\varepsilon}{\varepsilon_0}\right)^2}\right] \tag{6}$$

CEB-FIB (1993), adopted Sargin *et al.* model, modifying the expressions of the coefficients, to obtain Eq. (7) for the portion of the curve up to its point of inflection. The parameter E_0 is introduced, which corresponds to the slope of the secant line that joins the origin of the coordinate system, with the point of the stress-strain curve corresponding to the maximum compressive strength of the material, that is, the point of coordinates (f_0; ε_0). With another series of factors, the rest of the curve is obtained. Expressions for the determination of E and ε_0 are also introduced here.

$$f = f_0 \left[\frac{\left(\frac{E}{E_0}\right)\left(\frac{\varepsilon}{\varepsilon_0}\right) + B\left(\frac{\varepsilon}{\varepsilon_0}\right)^2}{1 + \left(\frac{E}{E_0} - 2\right)\left(\frac{\varepsilon}{\varepsilon_0}\right)}\right] \tag{7}$$

Van Gysel and Taerwe (1996), present their model, modifying the 1990 Model Code expression for the final part of the curve and proposing an expression for ε_0 as a function of f_0. Later, 2010 CEB-FIB Model Code (CEB-FIB 2010), discards the portion of the curve after the point of inflection and incorporates an expression for ε_0 as a function of the compressive strength of the concrete and its elastic modulus.

Other models deviate from these aforementioned lines of research. Almusallam and Alsayed

(1995), adapted the parameters of Eq. (8), from Richard and Abbott (1975), to fit the model to NC, HSC and LC.

$$f = \frac{(K-K_p)\varepsilon}{\left[1+\left(\frac{(K-Kp)\varepsilon}{f_0}\right)^n\right]^{\frac{1}{n}}} + K_p\varepsilon \tag{8}$$

There, K and K_p correspond to the initial and final slopes, respectively, of the stress-strain curve. That is, K is equal to the initial elastic modulus E of the material. Furthermore, n is a shape parameter of the curve, which depends on f, f_0, K, K_p, ε and ε_0.

Cui *et al.* (2012), developed a curve for structural concrete with lightweight aggregate (LWAC), which relates the compressive strength of the material y, with its specific strain x, which is presented in Eq. (9). The parameters ψ and ϕ depend on the volume, strength, form factor, and density of the lightweight aggregate and the strength and elastic modulus of the cement paste.

$$y = -\psi x^2 + 2\varphi x \tag{9}$$

This kind of model is very important for the study and understanding of a determined material's behaviour, in this case, in compression. That's why, several studies of this kind are in permanent development, for different types of concrete.

Zhao *et al.* (2017), investigated the compressive stress-strain curve of concrete made with coarse recycled concrete aggregate, after exposure to temperatures of between 20 and 800°C. A stress-strain model was developed for predicting the compressive stress-strain relationship of coarse recycled concrete after exposure.

Strukar *et al.* (2018), worked experimentally with rubberized concrete for improving stress-strain constitutive models. This is relevant because of the understanding of this kind of concrete behaviour. They evaluated the existing concrete models and proposed a new one, specifically adapted to this material's behaviour.

Liu *et al.* (2019), studied stress-strain relationship of plain and fibre-reinforced LWAC. Through an experimental campaign and its analysis, they could achieve a general stress-strain model adapted to plain LWAC and fibre-reinforced LWAC, by comparing and modifying the existing concrete models.

Similarly, Pimanmas and Saleem (2019), made a review of the existing concrete stress-strain models and evaluated their accuracy for modelling of polyethylene terephthalate fibre-reinforced polymer-confined concrete. They found that some characteristics could be well represented by the existing models, but some others don't. So, they proposed a new simple stress-strain model for this particular type of concrete.

Zeng *et al.* (2020), also studied confined concrete by application of polyethylene terephthalate fibre-reinforced polymer, which is made from recycled PET products and exhibits large rupture strain. They proposed a new stress-strain model by means of an experimental investigation on the stress-strain behaviour of polyethylene terephthalate fibre-reinforced polymer, confined normal, high, and ultra-high-strength concrete cylinders.

Yang *et al.* (2023) calculated the equations of the loading and unloading strain and established the equation of the stress-strain curve under a repetitive load of recycled aggregate concrete. This work was done to study the compressive mechanical properties and stress-strain relationships for this material. In this line of work, Liu *et al.* (2023) studied the stress-strain curve of recycled coarse aggregate concrete under uniaxial compression. They observed that the slope of the descending section of the stress-strain curve fluctuated after the addition of recycled coarse aggregate.

In order to evaluate the influence on concrete compressive behaviour of the incorporation of carbon nanotubes and steel fibres, Zhu *et al.* (2024), investigated the stress-strain curves of the composed material. A theoretical model for the uniaxial compressive constitutive relationship of concrete reinforced with carbon nanotubes and steel fibre was developed and important conclusions were drowned.

Recently, Li *et al.* (2024) investigated the axial stress-strain relationship of confined textile reinforced concrete to evaluate numerically the effectiveness of its use in repairing and strengthening concrete structures. They proposed a new closed-form algebraic expression for describing the confinement behaviour of textile-reinforced concrete by modifying Sargin's stress-strain relationship, which was introduced in Eq. (5).

As was shown, several mathematical models describe the compressive behaviour for different types of concretes, but no specific one for FCC has been developed, although some promising efforts that are continued here (Retamal and Rougier 2021).

In this work, a mathematical model of stress-strain curve for FCC is proposed by modifying that of CEB-FIB. Simple compression tests on FCC specimens of different mixes were conducted in order to observe the compression behaviour curve until failure. After them, stress-strain curves for FCC of different strengths were obtained. Then, by a statistical analysis of the experimentally obtained curves, mathematical expressions for determining the model's input variables were developed. Finally, the curves obtained by applying the proposed model were compared with the experimental ones, showing a high degree of correlation between them. This way, a mathematical model for representing the stress-strain curve for FCC was achieved.

2. Materials and methods

To develop a mathematical model of a stress-strain curve applicable to FCC, the ones reviewed in the previous section were analysed. It can be seen that some of them were developed for use in LWC, which is the type of concrete that FCC belongs to. Also, its compressive behaviour corresponds to this classification (ACI 2014a, Nguyen *et al.* 2017, Lim and Ozbakkaloglu 2014, Retamal and Rougier 2024). The CEB-FIB model is one of them, developed for its use in NC and LWC (CEB-FIB 2010). Furthermore, its input variables could be obtained from experimental load-displacement curves, applying statistical analysis. That is, the elastic modulus (E) and its strain to the maximum stress or strain to the peak (ε_0). Mathematical expressions for determining its input variables could be deducted from experimental campaigns, applying adjustment curves to the obtained results.

To obtain the experimental stress-strain curves, an experimental campaign was carried out. FCC cylindrical specimens of 150 mm (diameter)×300 mm (height) were made and cured as in the field, according to ASTM C-31 (ASTM 2022a) Standard.

Composite Portland Cement CPC 50 was used, with a specific density equal to 2.954, experimentally determined according to ASTM C188 (ASTM 2017); fine river sand, with a specific density in a saturated dry surface condition equal to 2.65, obtained according to ASTM C128 (ASTM 2015). To prepare the pre-formed foam, a commercial brand synthetic type of foaming agent was used, available in the local market. The mixtures used are shown in Table 1, and their design was conducted employing the compression strength prediction model for FCC developed by Retamal and Rougier.

Used mixes are shown in Table 1, and their design was conducted employing the strength

Table 1 Mix designs used for the experimental campaign

Mix design	Cement [kg/m³]	Water [kg/m³]	Sand [kg/m³]	Foam [kg/m³]
FCC-1	320.00	735.00	160.00	32.00
FCC-2	297.00	119.00	596.00	30.00
FCC-3	645.00	375.00	258.00	12.30
FCC-4	738.00	435.00	295.00	8.13
FCC-5	492.00	275.00	738.00	19.70
FCC-6	752.00	443.00	300.00	7.50
FCC-7	759.00	448.00	304.00	7.20
FCC-8	766.00	453.00	306.00	6.90
FCC-9	583.00	340.00	583.00	9.72
FCC-10	584.00	341.00	584.00	9.63
FCC-11	439.00	237.00	660.00	27.00
FCC-12	448.00	206.00	1030.00	18.00
FCC-13	684.00	406.00	684.00	4.17
FCC-14	561.00	331.00	867.00	5.61
FCC-15	565.00	333.00	903.00	5.36
FCC-16	566.00	335.00	906.00	5.24
FCC-17	702.00	347.00	843.00	3.86
FCC-18	870.00	345.00	435.00	2.60
FCC-19	1050.00	350.00	500.00	5.25
FCC-20	945.00	300.00	445.00	2.84
FCC-21	1116.00	378.00	536.00	1.67
FCC-22	1073.00	360.00	515.00	4.30

Fig. 1 Simple compression test (Test setup)

prediction model for FCC developed by Retamal and Rougier (2023).

Simple compression tests were carried out according to ASTM C39 (ASTM 2021) Standard, but curing time was extended to 56 days because the development of FCC mechanical strength requires more time compared to NC (Jones and McCarthy 2005). A compressometer was placed on each

Fig. 2 Simple compression test (Test specimen)

Table 2 Experimentally obtained results of compressive strength (f_C'), elastic modulus (E) and specific strain corresponding to the maximum stress reached (ε_0), for each FCC mix design

Mix design	f_C' [MPa]	E [GPa]	ε_0 [$\times 10^4$]
FCC-1	1.20	15.32	0.80
FCC-2	1.60	6.58	4.00
FCC-3	2.17	12.56	2.29
FCC-4	4.32	16.48	3.33
FCC-5	4.33	20.95	2.30
FCC-6	4.89	13.95	4.58
FCC-7	5.07	14.48	8.75
FCC-8	5.29	12.77	4.36
FCC-9	5.50	6.08	7.45
FCC-10	5.56	23.66	2.79
FCC-11	6.43	10.56	7.84
FCC-12	12.64	19.96	10.00
FCC-13	12.76	24.38	4.99
FCC-14	14.35	18.72	11.76
FCC-15	14.90	18.94	10.56
FCC-16	15.12	17.40	13.69
FCC-17	22.00	18.07	11.65
FCC-18	39.61	27.11	27.43
FCC-19	40.90	27.13	26.68
FCC-20	44.96	29.03	26.97
FCC-21	46.94	29.25	28.05
FCC-22	47.34	28.65	27.63

specimen, with 3 potentiometers to measure the deformation and a load cell to obtain the applied force values. An HBM QuantumX MX840B unit was used, connected to a computer with CatmanEasy software, for continuous data measurement. The test configuration of a specimen is

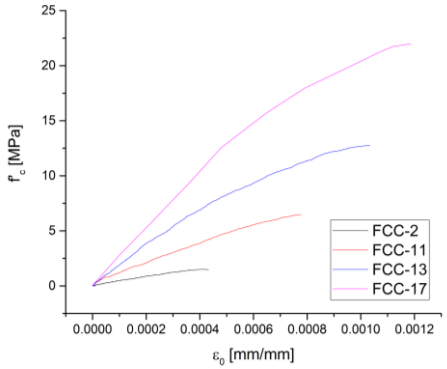

Fig. 3 Example of experimentally obtained stress-strain curves of mixes FCC-2, FCC-11, FCC-13 and FCC-17

Table 3 Comparison of models for elastic modulus (E) determination (Example of procedure with 3 mix design)

E [GPa]	FCC-2	FCC-11	FCC-13
$4300\gamma^{1.5}\sqrt{f_C'}$ (ACI 2014a)	1.62	4.98	9.90
$420(f_C')^{1.18}$ (Jones and McCarthy 2005)	0.68	3.79	8.38
$990(f_C')^{0.67}$ (Jones and McCarthy 2005)	1.30	3.45	5.42
$\eta_E E$ (CEB-FIB 2010)	2.73	7.50	14.98
$4700\sqrt{f_C'}$ (ACI 2014b)	5.75	11.94	16.71
$6326\gamma^{1.5}\sqrt{f_C'}$ (Byun *et al.* 1998)	2.39	7.32	14.56
$9100(f_C')^{0.33}$ (Rowe *et al.* 1987)	10.40	16.83	21.02
$5700\gamma^{1.5}\sqrt{f_C'}$ (Kamara *et al.* 2008)	6.97	14.48	20.27
Present work (experimental results)	6.58	10.56	24.38

shown in Figs. 1 and 2.

The load application was carried out with a Shimadzu Universal Testing Machine, with a capacity of 1000 kN.

The experimentally obtained load-deflection curves were processed to obtain the stress strain curves and, this way, study the behaviour of the FCC at simple compression.

3. Results and discussion

The experimentally obtained results are summarized in Table 2, where: compressive strength (f_C'), elastic modulus (E), and specific strain corresponding to the maximum stress reached (ε_0), for each dosage of FCC are displayed. There, it can be seen the different mechanical characteristics of the used mixes. Load-displacement curves obtained for each sample of the material were processed to obtain the respective stress-strain curves. Some examples of them are presented in Fig. 3.

To compare the compressive behaviour of the different FCC mixes, the obtained curves were normalized, dividing the values of the specific deformation and the tension obtained at each point, by their respective maximum values. This way it can be seen the similar compressive behaviour of

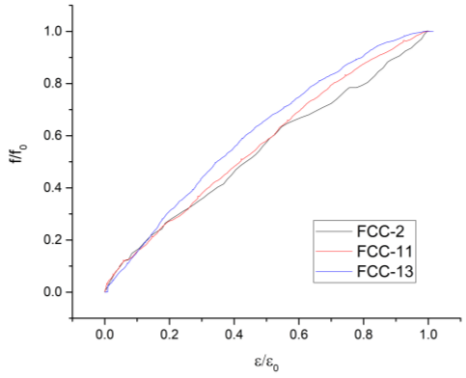

Fig. 4 Normalized curves comparison example of mixes 2, 11 and 13

FCC with other lightweight concretes, as observed by Nguyen *et al.* (2019). That is a quasi-static constant slope from the beginning of the application of the load until the zone before the failure is observed. This shows the brittle behaviour of the material and the way of failure.

The values of the elastic modulus (E) experimentally obtained in the present work for the different mix designs were compared with prediction models from various authors, as can be seen on Table 3 (ACI 2014a, Byun *et al.* 1998, CEB-FIB 2010, ACI 2014b, Jones and McCarthy 2005, Kamara *et al.* 2008, Koz lowski and Kadela 2018, McCormick 1967, Rowe *et al.* 1987, Tada 1986, Van Gysel and Taerwe 1996).

It is observed that the values obtained through the evaluated expressions present a significant dispersion, which is expected since models conceived through tests on various types of concrete were evaluated. Even in the cases of authors who worked with FCC, they did not do so with materials with the same characteristics as those used in this work. Therefore, the values of E obtained experimentally were analysed, and a prediction model of the elastic modulus was obtained for FCC made with cement, water, pre-formed foam, and sand, of different densities and characteristic resistances, through a potential curve of adjustment.

For each test specimen, the elastic modulus (E) was determined, according to the normative ASTM C469 ASTM (2022b), and the obtained results are presented over the "y" axis, in Fig. 4. On the x axis, the values for the corresponding compressive strength (f_C') were placed. Then, through statics analysis, a potential fitting curve was adjusted to this data, because it was the one with a higher value for the correlation coefficient (R^2), which was equal to 0.66, indicating a high relationship between the proposed analytical expression and the experimental data. This observation is in coincidence with other authors proposed equation to related this two variables (ACI 2014a, Byun *et al.* 1998, CEB-FIB 2010, ACI 2014b, Jones and McCarthy 2005, Kamara *et al.* 2008, Koz lowski and Kadela 2018, McCormick 1967, Rowe *et al.* 1987, Tada 1986, Van Gysel and Taerwe 1996).

As can be seen in Fig. 5, the expression obtained for the elastic modulus as a function of the material's strength is equal to

$$E = 9.4372 f_C'^{\,0.2822} \tag{10}$$

In the same way, the procedure to determine the specific deformation of the material peak was carried out. Firstly, the expressions of different authors (Popovics 1973, CEB-FIB 1993, Sargin *et al.* 1971, Tomaszewicz 1984, Carreira and Chu 1985, Wee *et al.* 1996) were evaluated, comparing

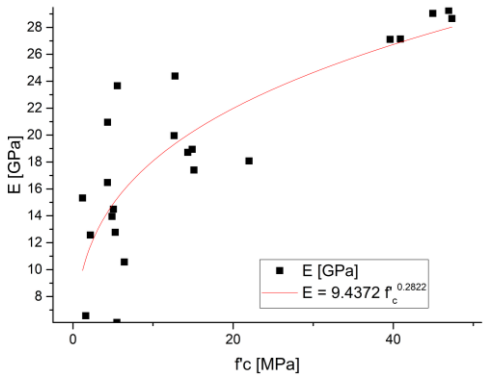

Fig. 5 Potential fitting curve for experimental values of f_C' vs. E

Table 4 Specific strain at peak strength (ε_0) models evaluated for FCC (Example of procedure with 3 mix design)

ε_0	FCC-2	FCC-11	FCC-13
$735(f_C')^{0.25}$ (ACI 2014a)	0.00083	0.00117	0.00139
Constant (Sargin *et al.* 1971)	0.0024	0.0024	0.0024
$700(f_C')^{0.31}$ (Tomaszewicz 1984)	0.00081	0.00125	0.00154
$1.68 + 7.1f_C'$ (Carreira and Chu 1985)	0.0001	0.0005	0.0009
$780(f_C')^{1/4}$ (Wee *et al.* 1996)	0.00088	0.00124	0.00147
$-1.3\frac{f_C'+8}{E}$ (CEB-FIB 2010)	0.00546	0.00251	0.00179
Present work (experimental results)	0.00040	0.00078	0.00050

them with the experimental results. And example of this procedure, with 3 mix designs, is presented in Table 4.

In a similar way to what happened in the case of the elastic modulus, the values obtained by the considered models differ from those obtained experimentally. In the case of the peak strain (ε_0), there are no specific models for its prediction developed for FCC. Therefore, the expressions considered correspond to different types of concrete, none of them, FCC. The experimental data was analysed, which is represented in Fig. 6.

The values for the specific strain at the point of maximum compressive strength (ε_0) were also determined from the experimentally obtained data. In the Cartesian graph of Fig. 6 these values can be seen in the *y* axis, together with their corresponding compressive strength (f_C'), placed in the *x* axis.

The potential fitting curve was again the one with a higher value for R^2, equal to 0.95.

Showing the correlation between these values, and the proposed mathematical expression, in coincidence with the observations of other studies (Popovics 1973, Tomaszewicz 1984, Wee *et al.* 1996). The expression obtained is presented in Eq. (11)

$$\varepsilon_0 = 1.2370\, f_C'^{0.8143} \times 10^{-4} \tag{11}$$

In this way, the model for the determination of the specific strain corresponding to the peak stress (ε_0) for FCC was obtained, suitable for mix designs of various densities and resistances.

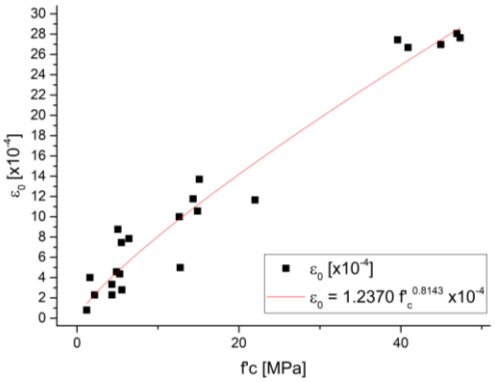

Fig. 6 Potential fitting curve for experimental values of f_C' vs. ε_0

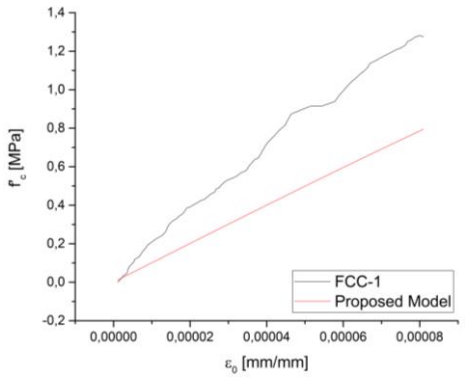

Fig. 7 Evaluation of the proposed model (Against mix FCC-1)

As discussed, to generate the mathematical model of the FCC stress-strain curve, the CEB-FIB Model Code 2010 mathematical expression was adopted (CEB-FIB 2010). Modifying the equation for the determination of the elastic modulus (E) and the maximum stress peak (ε_0), by the ones developed in this work. Furthermore, the secant elastic modulus (E_0) could be obtained within the elastic modulus (E) and the maximum stress peak (ε_0). The complete analytical model for FCC is compiled in Eqs. (12) to (15)

$$f_c = f_c' \left[\frac{\left(\frac{E}{E_0}\right)\left(\frac{\varepsilon}{\varepsilon_0}\right) - \left(\frac{\varepsilon}{\varepsilon_0}\right)^2}{1 + \left(\frac{E}{E_0} - 2\right)\left(\frac{\varepsilon}{\varepsilon_0}\right)} \right] \tag{12}$$

$$E = 9.4372 {f_c'}^{0.2822} \tag{13}$$

$$\varepsilon_0 = 1.2370 {f_c'}^{0.8143} \times 10^{-4} \tag{14}$$

$$E_0 = \frac{f_c'}{\varepsilon_0} \tag{15}$$

The proposed model was evaluated by comparing it with the experimentally obtained results. This procedure is shown next in Figs. 7 to 19, where superimposed graphs of the curves determined

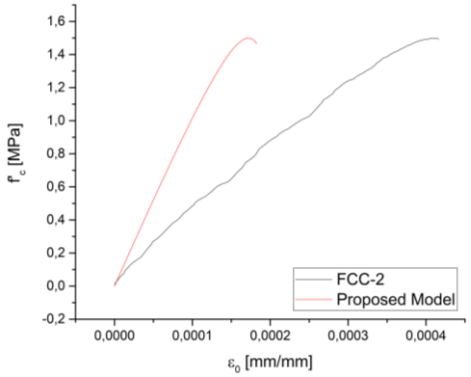

Fig. 8 Evaluation of the proposed model (continuation) (Against mix FCC-2)

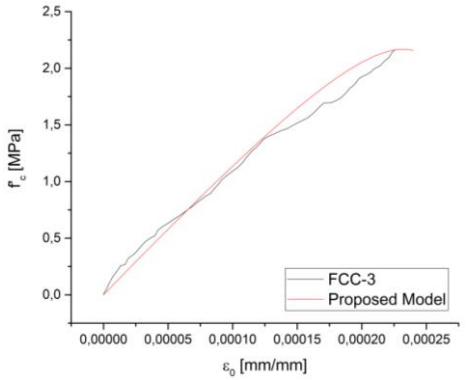

Fig. 9 Evaluation of the proposed model (continuation) (Against mix FCC-3)

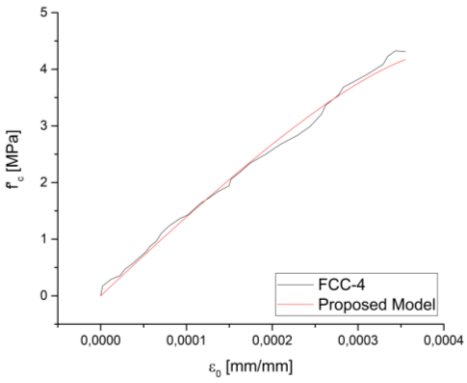

Fig. 10 Evaluation of the proposed model (continuation) (Against mix FCC-4)

experimentally against those obtained through the application of the proposed model are presented.

In general, a good approximation of the curve generated by the proposed model to the experimentally obtained is graphically observed.

The theoretical values obtained with the proposed model for the compressive strength (f'_{cT}) were compared with the experimentally obtained ones (f'_c). Also, statistical analysis was conducted, as is

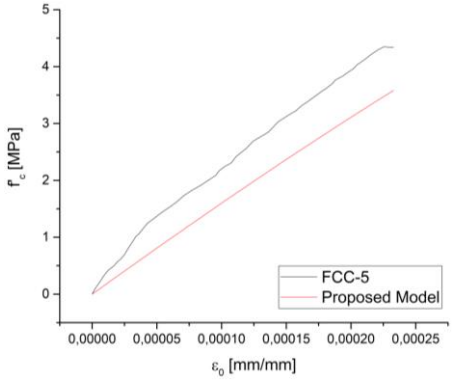

(a) Against mix FCC-5

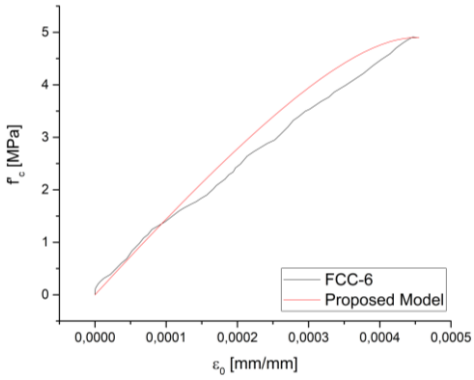

(b) Against mix FCC-6

Fig. 11 Evaluation of the proposed model (continuation)

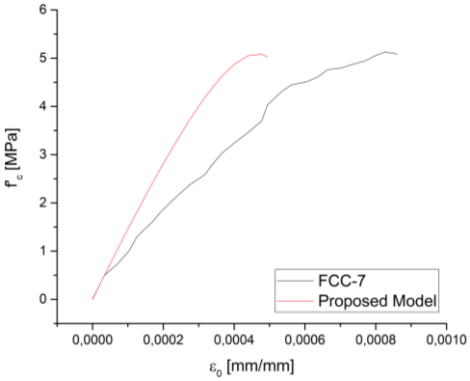

(a) Against mix FCC-7

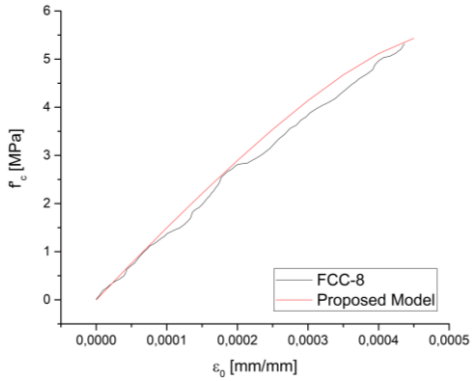

(b) Against mix FCC-8

Fig. 12 Evaluation of the proposed model (continuation)

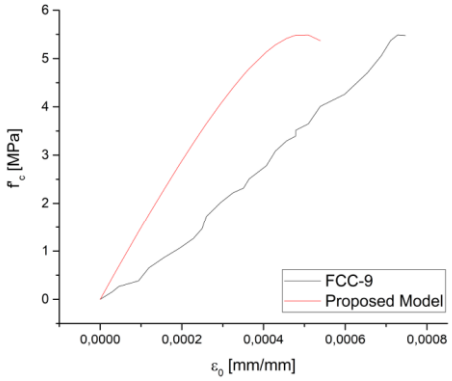

(a) Against mix FCC-9

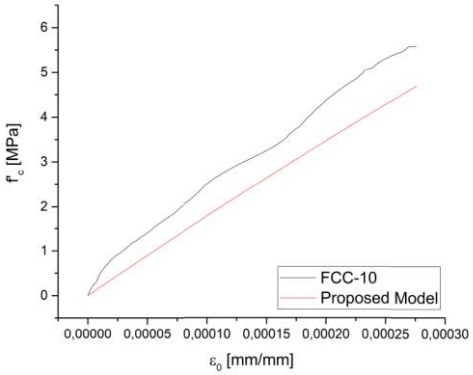

(b) Against mix FCC-10

Fig. 13 Evaluation of the proposed model (continuation)

shown in Table 5.

The statistical analysis of the relationship between experimentally obtained values and

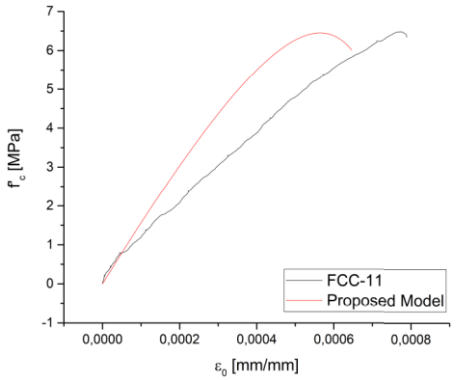

(a) Against mix FCC-11

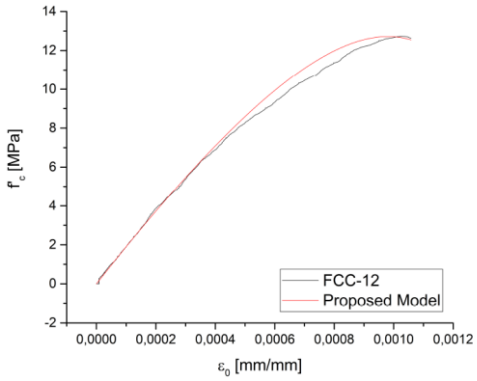

(b) Against mix FCC-12

Fig. 14 Evaluation of the proposed model (continuation)

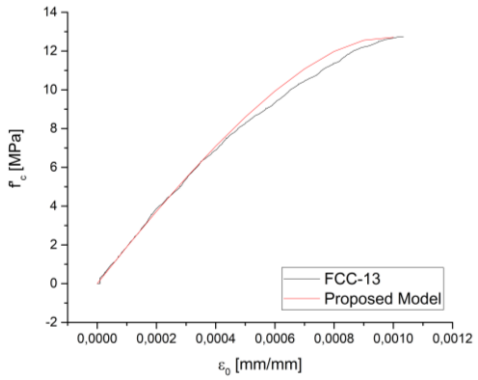

(a) Against mix FCC-13

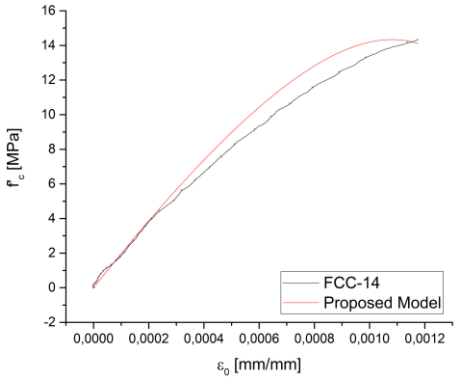

(b) Against mix FCC-14

Fig. 15 Evaluation of the proposed model (continuation)

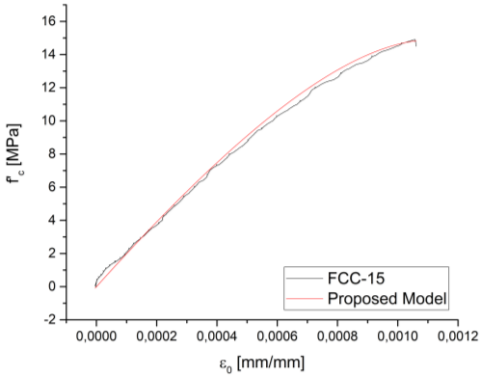

(a) Against mix FCC-15

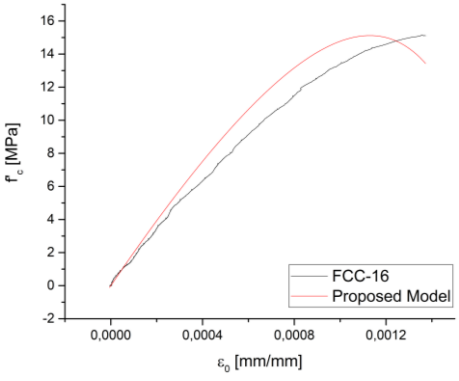

(b) Against mix FCC-16

Fig. 16 Evaluation of the proposed model (continuation)

theoretically proposed equations, for the elastic modulus (E) and peak-specific strength (ε_0), was conducted using the coefficient of determination (R^2). In the same way, the coefficient of

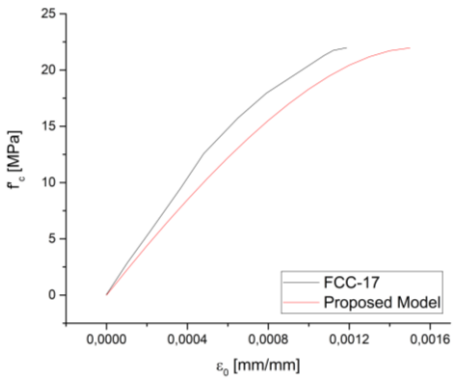

(a) Against mix FCC-17

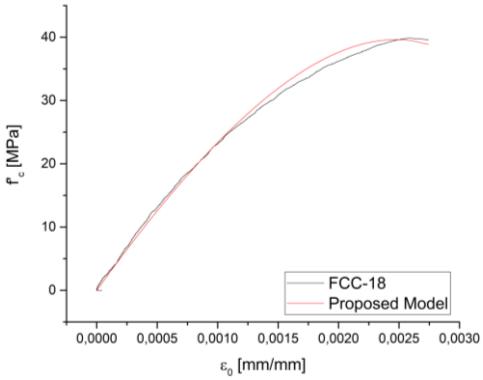

(b) Against mix FCC-18

Fig. 17 Evaluation of the proposed model (continuation)

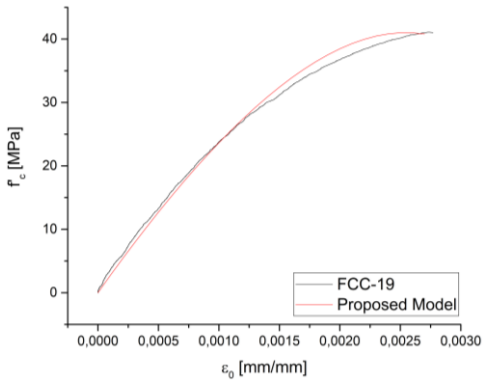

(a) Against mix FCC-19

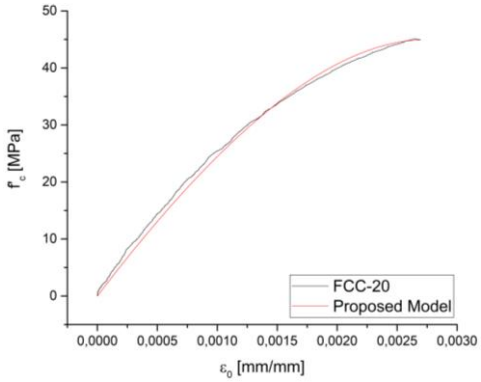

(b) Against mix FCC-20

Fig. 18 Evaluation of the proposed model (continuation)

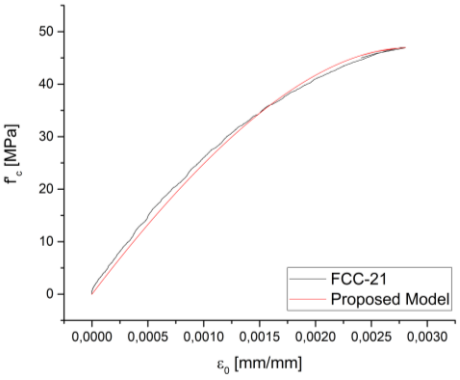

(a) Against mix FCC-21

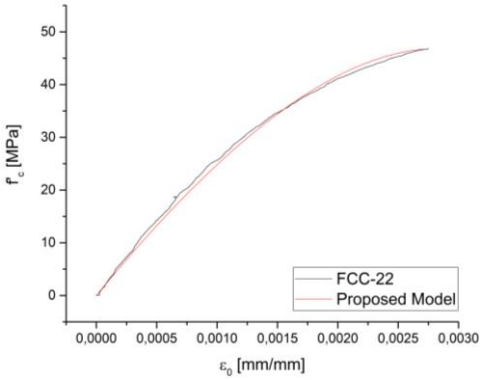

(b) Against mix FCC-22

Fig. 19 Evaluation of the proposed model (continuation)

determination (R^2) between the experimental values of compression strength (f_c') and those obtained through the proposed model (f_{cT}') was calculated equal to 0.99. Furthermore, the correlation

Table 5 Comparison between the experimental values of compression strength (f_c') and those obtained through the proposed model (f_{cT}')

Mix design	f_c' [MPa]	f_{cT}' [GPa]	Absolute error [MPa]	Percentage error [%]
FCC-1	1,20	0,79	0,41	-34,17
FCC-2	1,60	1,50	0,10	-6,25
FCC-3	2,17	2,17	0,00	0,00
FCC-4	4,32	4,17	0,15	-3,47
FCC-5	4,33	3,48	0,85	-19,63
FCC-6	4,89	4,90	0,01	0,20
FCC-7	5,07	5,08	0,01	0,20
FCC-8	5,29	5,19	0,10	-1,89
FCC-9	5,50	5,48	0,02	0,31
FCC-10	5,56	4,69	0,87	-15,65
FCC-11	6,43	6,45	0,02	0,31
FCC-12	12,64	12,70	0,06	0,47
FCC-13	12,76	12,74	0,02	-0,16
FCC-14	14,35	14,32	0,03	-0,21
FCC-15	14,90	14,83	0,07	-0,47
FCC-16	15,12	15,11	0,01	-0,07
FCC-17	22,00	15,11	0,01	-0,07
FCC-18	39,61	39,55	0,06	-0,15
FCC-19	40,90	40,89	0,01	-0,02
FCC-20	44,96	44,94	0,02	-0,04
FCC-21	46,94	46,92	0,02	-0,04
FCC-22	47,34	47,24	0,10	-0,21

coefficient was determined equal to 0.99. Also, a mean absolute error of 0.15 MPa and a mean absolute percentage error of 3.77 % were obtained. Witch shows the effectiveness of the proposed model in representing the compressive behaviour of FCC.

The main limitation of the conducted study lies in adopting the descending portion of the compressive behaviour curve for FCC from the CEB-FIB model. However, this segment is the least relevant in terms of material strength properties and simulation of its behaviour, as demonstrated through the proposed simplification for its consideration between successive editions of the Model Code (CEB-FIB 1993, 2010). Furthermore, the study of material behaviour up to its peak strength under specific stresses has proven to be relevant for understanding their response to external solicitations (Cui *et al.* 2012). As future work, conducting studies addressing the measurement of the entire curve is proposed.

4. Conclusions

In the present work, an analytical model of the stress-strain curve at compression for FCC was

obtained, through an experimental campaign and the analysis of its results. The following conclusions were obtained:

- Conducted experimental work confirmed the compression behaviour of FCC as lightweight concrete.
- It is possible to use the curve presented in the CEB-FIB 2010 Model Code, to represent the compressive behaviour of foamed cellular concrete. However, the values proposed in this model for the elastic modulus (E) and the specific strain to the peak (ε_0) do not agree with the experimentally obtained results.
- It was observed that the elastic modulus (E) of FCC increases with increasing compressive strength (f_c'). Furthermore, the relationship between these variables behaves as a power-type function.
- Similarly, the strain at peak (ε_0) increases with the compressive strength (f_c') of the FCC, and its relationship can be expressed through a power function.
- The analytical model of the CEB-FIB Model Code 2010, modified by these expressions determined in the present work, achieves an adequate approximation to the compression behaviour of the foamed cellular concrete experimentally determined, for the studied mix designs.

Acknowledgements

The authors gratefully acknowledge the support for this research from GEMA research group of the UTN FRCU, "Premoldeados Salamanca" enterprise and "Ferrocement" enterprise.

Conflict of interest

The authors declare that they have no conflict of interest.

References

ACI (2014a), 523.3R-14: Guide for Cellular Concretes above 50 lb/ft^3 (800 kg/m^3), American Concrete Institute, Farmington Hills, MI, USA.

ACI (2014b), ACI 318-14: Building Code Requirements for Structural Concrete: Commentary on Building Code Requirements for Structural Concrete (ACI 318R-14): An ACI Report, American Concrete Institute, Farmington Hills, MI, USA.

Almasabha, G., Alshboul, O., Shehadeh, A. and Almuflih, A.S. (2022), "Machine learning algorithm for shear strength prediction of short links for steel buildings", *Build.*, **12**(6), 775. https://doi.org/10.3390/buildings12060775.

Almusallam, T. and Alsayed, S. (1995), "Stress-strain relationship of normal, high-strength and lightweight concrete", *Mag. Concrete Res.*, **47**(170), 39-44. https://doi.org/10.1680/macr.1995.47.170.39.

Alshboul, O., Almasabha, G., Shehadeh, A., Al Hattamleh, O. and Almuflih, A.S. (2022a), "Optimization of the structural performance of buried reinforced concrete pipelines in cohesionless soils", *Mater.*, **15**(12), 4051. https://doi.org/10.3390/ma15124051.

Alshboul, O., Almasabha, G., Shehadeh, A., Mamlook, R.E.A., Almuflih, A.S. and Almakayeel, N.(2022b), "Machine learning-based model for predicting the shear strength of slender reinforced concrete beams

without stirrups", *Build.*, **12**(8), 1166. https://doi.org/10.3390/buildings12081166.
Amran, Y.M., Farzadnia, N. and Ali, A.A. (2015), "Properties and applications of foamed concrete; a review", *Constr. Build. Mater.*, **101**, 990-1005. https://doi.org/10.1016/j.conbuildmat.2015.10.112.
ASTM (2015), C128: Standard Test Method for Relative Density (Specific Gravity) and Absorption of Fine Aggregate, ASTM International, West Conshohocken, PA, USA.
ASTM (2017), C188: Standard Test Method for Density of Hydraulic Cement, ASTM International, West Conshohocken, PA, USA.
ASTM (2021), C39: Standard Test Method for Compressive Strength of Cylindrical Concrete Specimens, ASTM International, West Conshohocken, PA, USA.
ASTM (2022a), C31: Practice for Making and Curing Concrete Test Specimens in the Field, ASTM International, West Conshohocken, PA, USA.
ASTM (2022b), C469: Test Method for Static Modulus of Elasticity and Poissons Ratio of Concrete in Compression, ASTM International, West Conshohocken, PA, USA.
Brady, K., Watts, G. and Jones, M. (2001), *Application Guide AG39: Specification for Foamed Concrete*, Highways Agency and Transport Research Laboratory, Wokingham, UK.
Byun, K., Song, H., Park, S. and Song, Y. (1998), "Development of structural lightweight foamed concrete using polymer foam agent", *ICPIC-98*, Bologna, Italy, September.
Carreira, D.J. and Chu, K.H. (1985), "Stress-strain relationship for plain concrete in compression", *J. Proc.*, **82**, 797-804.
CEB-FIB (1993), Model Code 1990: Design Code, 213-214, International Federation for Structural Concrete, Lausanne, Switzerland.
CEB-FIB (2010), Model Code for Concrete Structures 2010, International Federation for Structural Concrete, Lausanne, Switzerland.
Chica, L. and Alzate, A. (2019), "Cellular concrete review: New trends for application in construction", *Constr. Build. Mater.*, **200**, 637-647. https://doi.org/10.1016/j.conbuildmat.2018.12.136.
Cui, H., Lo, T.Y., Memon, S.A., Xing, F. and Shi, X. (2012), "Experimental investigation and development of analytical model for pre-peak stress-strain curve of structural lightweight aggregate concrete", *Constr. Build. Mater.*, **36**, 845-859. https://doi.org/10.1016/j.conbuildmat.2012.06.041.
Hsu, L. and Hsu, C.T. (1994), "Complete stress-strain behaviour of high-strength concrete under compression", *Mag. Concrete Res.*, **46**(169), 301-312. https://doi.org/10.1680/macr.1994.46.169.301.
Jones, M. and McCarthy, A. (2005), "Preliminary views on the potential of foamed concrete as a structural material", *Mag. Concrete Res.*, **57**(1), 21-31. https://doi.org/10.1680/macr.2005.57.1.21.
Kamara, M.E., Novak, L.C. and Rabbat, B.G. (2008), *Notes on ACI 318-08, Building Code Requirements for Structural Concrete: With Design Applications*, Portland Cement Association, Washington, D.C., USA.
Kozlowski, M. and Kadela, M. (2018), "Mechanical characterization of lightweight foamed concrete", *Adv. Mater. Sci. Eng.*, **2018**, 1-9. https://doi.org/10.1155/2018/6801258.
Li, Y., Yin, S., Zhao, K., Li, S., Wang, W. and Sheng, J. (2024), "A new modified stress-strain model for concrete confined with textile reinforced concrete composites", *J. Build. Eng.*, **86**, 108858. https://doi.org/10.1016/j.jobe.2024.108858.
Lim, J.C. and Ozbakkaloglu, T. (2014), "Stress-strain model for normal-and light-weight concretes under uniaxial and triaxial compression", *Constr. Build. Mater.*, **71**, 492-509. https://doi.org/10.1016/j.conbuildmat.2014.08.050.
Liu, B., Zhang, B., Wang, Z.Z. and Bai, G.L. (2023), "Study on the stress-strain full curve of recycled coarse aggregate concrete under uniaxial compression", *Constr. Build. Mater.*, **363**, 129884. https://doi.org/10.1016/j.conbuildmat.2022.129884.
Liu, X., Wu, T. and Liu, Y. (2019), "Stress-strain relationship for plain and fibre-reinforced lightweight aggregate concrete", *Constr. Build. Mater.*, **225**, 256-272. https://doi.org/10.1016/j.conbuildmat.2019.07.135.
Lu, Z.H. and Zhao, Y.G. (2010), "Empirical stress-strain model for unconfined high-strength concrete under uniaxial compression", *J. Mater. Civil Eng.*, **22**(11), 1181-1186. https://doi.org/10.1061/(ASCE)MT.1943-5533.0000095.

McCormick, F.C. (1967), "Rational proportioning of preformed foam cellular concrete", *J. Proc.*, **64**, 104-110. https://doi.org/10.14359/7547.

Narayanan, N. and Ramamurthy, K. (2000), "Structure and properties of aerated concrete: A review", *Cement Concrete Compos.*, **22**(5), 321-329. https://doi.org/10.1016/S0958-9465(00)00016-0.

Nguyen, T.T., Bui, H.H., Ngo, T.D. and Nguyen, G.D. (2017), "Experimental and numerical investigation of influence of air-voids on the compressive behaviour of foamed concrete", *Mater. Des.*, **130**, 103-119. https://doi.org/10.1016/j.matdes.2017.05.054.

Nguyen, T.T., Bui, H.H., Ngo, T.D., Nguyen, G.D., Kreher, M.U. and Darve, F. (2019), "Amicromechanical investigation for the effects of pore size and its distribution on geopolymer foam concrete under uniaxial compression", *Eng. Fract. Mech.*, **209**, 228-244. https://doi.org/10.1016/j.engfracmech.2019.01.033.

Pimanmas, A. and Saleem, S. (2019), "Evaluation of existing stress-strain models and modeling of PET FRP-confined concrete", *J. Mater. Civil Eng.*, **31**(12), 04019303. https://doi.org/10.1061/(ASCE)MT.1943-5533.0002941.

Popovics, S. (1973), "A numerical approach to the complete stress-strain curve of concrete", *Cement Concrete Res.*, **3**(5), 583-599. https://doi.org/10.1016/0008-8846(73)90096-3.

Retamal, F.A. and Rougier, V.C. (2021), "Experimental study and development of an analytical model of stress-strain curve for foamed cellular concrete in uniaxial compression", *26 Argentine Conference on Structural Engineering*.

Retamal, F.A. and Rougier, V.C. (2022), "Mechanical behaviour, properties and characteristics of foamed cellular concrete: A review", *Adv. Mater. Res.*, **1170**, 61-85. https://doi.org/10.4028/p-ds0fcq.

Retamal, F.A. and Rougier, V.C. (2023), "Strength prediction model for foamed cellular concrete", *J. Mech. Mater. Struct.*, **18**(4), 427-443. https://doi.org/10.2140/jomms.2023.18.427.

Retamal, F.A. and Rougier, V.C. (2024), "Mechanical behavior of reinforced concrete hybrid beams made with normal concrete, foamed cellular concrete and fiber reinforced foamed cellular concrete", *Innov. Infrastr. Solut.*, **9**(1), 11. https://doi.org/10.1007/s41062-023-01258-8.

Richard, R.M. and Abbott, B.J. (1975), "Versatile elastic-plastic stress-strain formula", *J. Eng. Mech. Div.*, **101**(4), 511-515. https://doi.org/10.1061/JMCEA3.0002047.

Rowe, R., Somerville, G. and Beeby, A. (1987), *Handbook to British Standard BS8110: 1985: Structural Use of Concrete*, Palladian, London, UK.

Sargin, M., Ghosh, S.K. and Handa, V. (1971), "Effects of lateral reinforcement upon the strength and deformation properties of concrete", *Mag. Concrete Res.*, **23**(75-76), 99-110. https://doi.org/10.1680/macr.1971.23.76.99.

Strukar, K., Kalman Šipoš, T., Dokšanović, T. and Rodrigues, H. (2018), "Experimental study of rubberized concrete stress-strain behavior for improving constitutive models", *Mater.*, **11**(11), 2245. https://doi.org/10.3390/ma11112245.

Sun, C., Zhu, Y., Guo, J., Zhang, Y. and Sun, G. (2018), "Effects of foaming agent type on the workability, drying shrinkage, frost resistance and pore distribution of foamed concrete", *Constr. Build. Mater.*, **186**, 833-839. https://doi.org/10.1016/j.conbuildmat.2018.08.019.

Tada, S. (1986), "Material design of aerated concrete—An optimum performance design", *Mater. Struct.*, **19**(1), 21-26. https://doi.org/10.1007/BF02472306.

Tarawneh, A., Almasabha, G., Alawadi, R. and Tarawneh, M. (2021), "Innovative and reliable model for shear strength of steel fibers reinforced concrete beams", *Struct.*, **32**, 1015-1025. https://doi.org/10.1016/j.istruc.2021.03.081.

Tomaszewicz, A. (1984), "Betongens arbeidsdiagram", *SINTEF Report STF A*, **65**, 84065.

Van Gysel, A. and Taerwe, L. (1996), "Analytical formulation of the complete stress-strain curve for high strength concrete", *Mater. Struct.*, **29**(9), 529-533. https://doi.org/10.1007/BF02485952.

Wang, P., Shah, S. and Naaman, A. (1978), "Stress-strain curves of normal and lightweight concrete in compression", *J. Proc.*, **75**, 603-611. https://doi.org/10.14359/10973.

Wee, T., Chin, M. and Mansur, M. (1996), "Stress-strain relationship of high-strength concrete in compression", *J. Mater. Civil Eng.*, **8**(2), 70-76. https://doi.org/10.1061/(ASCE)0899-1561(1996)8:2(70).

Yang, H., Fang, J., Jiang, J., Li, M. and Mei, J. (2023), "Compressive stress-strain curve of recycled concrete

under repeated loading", *Constr. Build. Mater.*, **387**, 131598. https://doi.org/10.1016/j.conbuildmat.2023.131598.

Zeng, J.J., Ye, Y.Y., Gao, W.Y., Smith, S.T. and Guo, Y.C. (2020), "Stress-strain behavior of polyethylene terephthalate fiber-reinforced polymer-confined normal-, high-and ultra high-strength concrete", *J. Build. Eng.*, **30**, 101243. https://doi.org/10.1016/j.jobe.2020.101243.

Zhao, H., Wang, Y. and Liu, F. (2017), "Stress-strain relationship of coarse RCA concrete exposed to elevated temperatures", *Mag. Concrete Res.*, **69**(13), 649-664. https://doi.org/10.1680/jmacr.16.00333.

Zhu, P., Jia, Q., Li, Z., Wu, Y. and Ma, Z.J. (2024), "Theoretical model for the stress-strain curve of CNT-reinforced concrete under uniaxial compression", *Build.*, **14**(2), 418. https://doi.org/10.3390/buildings14020418.

CC